Journal of the Serbian Chemical Society
JSCS-info@shd.org.rs • www.shd.org.rs/JSCS
J. Serb. Chem. Soc. *83* (2) 221–236 (2018)
JSCS–5070
UDC 546.47/.48–31:546.26–162+542.92+667.281:504.054–039.7
Original scientific paper

ZnO/CdO/reduced graphene oxide and its high catalytic performance towards degradation of the organic pollutants

HODA MIRZAZADEH and MARYAM LASHANIZADEGAN*

Department of Chemistry, Faculty of Physics and Chemistry, Alzahra University, P. O. Box 1993893973, Tehran, Iran

(Received 30 June, revised 10 August, accepted 11 August 2017)

Abstract: ZnO/CdO nanoparticles on the reduced graphene oxide (ZnO/CdO/ /reduced graphene oxide) were prepared by a hydrothermal process. The structure and morphology were investigated by FTIR, UV-Vis, XRD, EDX, DRS, SEM and TEM. The sonocatalytic properties of ZnO/CdO/reduced graphene oxide were evaluated in the degradation of mefenamic acid (MEF), methyl orange (MO), rhodamin (RhB) and 4-nitroaniline (4-NA). Based on the results, the effective and high efficiency of the degradation of azo dyes (MO: 84 %, RhB: 80 %), MEF: 93 % and 4-NA: 95 % were observed in 120 min after the beginning of the reactions. The effects of factors such as ZnO/CdO/reduced graphene oxide dosage, initial concentration of organic pollutant, ultrasonic power and the presence of ROS (reactive oxygen species) scavengers on the degradation efficiency were reviewed. It was found that the presence of scavengers suppressed the sonocatalytic degradation efficiency. This research indicates the as-prepared nanocomposites exhibit much higher catalytic activity than ZnO/CdO nanoparticles and reduce graphene oxide (rGO).

Keywords: sonocatalysis; 4-nitroaniline; degradation; mefenamic acid; azo dyes; ultrasonic waves; scavengers.

INTRODUCTION

In recent years NSIDS (non-steroidal anti-inflammatory drugs) have been widely used. MEF, a common NSIDS, is one of diphenylamine derivative pollutant. Diphenylamine derivative pollutants release their toxins in waters. These compounds cannot be removed from waste waters by conventional methods.[1–4] Beside them, azo dyes and nitro aromatic compounds are among the most important groups of industrial chemicals.[5] Due to the growing use of these compounds, the resulted pollution of waste waters is becoming a critical concern. These pollutants have unfavourable effects on the environment and humans.

* Corresponding author. E-mail: m_lashani@alzahra.ac.ir
https://doi.org/10.2298/JSC170630097M

Thus removal of these pollutants from waste waters is essential.[6–8] In recent years, semiconductor nanoparticles have received more attention due to their unique catalytic properties. These properties make them suitable material for potential applications in various fields. They include waste water treatment, electrochemical sensors, drug delivery and antibacterial effects.[9–11] However these semiconductor nanoparticles have some limitations, because their small size and large surface area can lead to particle-particle aggregation, making the physical handling of nanoparticles difficult in liquid and dry forms.[12–14] Graphene as a two--dimensional carbon nanomaterial has the properties such as fast electron transportation, high aspect ratio, high mobility of charge carries and so on.[15] With these properties, graphene oxide is a promising support. Combining the semiconductor nanoparticles with graphene is considered a more preferable technique. Nanocomposites with semiconductor nanomaterial are used for various applications such as waste water treatment, bio nanoelectronic devices and capacitors.[16–18] The conjugated structure and functional groups at the edge of graphene, like carboxyl and carbonyl, can increase its interaction with semiconductors. When strong interaction occur, the electrons in the conduction band of semiconductors transfer to graphene and this process can lead to the electron hole separation and to the enhanced efficiency of the nanocomposites.[19] There are several studies about the synthesis and properties of graphene- semiconductor nanoparticles.[20–22] Lv *et al.* prepared ZnO/rGO composite which has enhanced photocatalytic properties to degrade methylene blue.[23] Han *et al.* synthesized CdS/ZnO/graphene composite and they found high efficiency of the photoelectrochemical activity of the nanocomposite under solar irradiation.[24] Ahmad *et al.* investigated the sonophotocatalytic degradation of RhB using ZnO/CNT composites.[25] Zhu *et al.* fabricated PbSe–TiO_2–graphene and applied it as sonocatalyst for the decolourization of industrial dyes.[26]

As one of the most promising semiconductors, ZnO has got the extensive attention due to its high oxidative capacity, low cost and easy availability.[27–29] The technological applications of ZnO are limited by its band gap (3.0–3.8 eV),[30] and by the requirement of the UV light to create the electron-hole pairs. Furthermore, CdO is an important semiconductor with band gap of 2.2 eV.[31] CdO has the advantage of low resistivity, and high transmittance in the visible region. These properties make it useful for the variety of applications such as photodiodes, photovoltaic cells, liquid crystal displays, catalyst, *etc.*[32,33] The coupling of ZnO and CdO can reduce the band gap, extending the absorption range to the visible light region, leading to the electron-hole separation and consequently achieving higher activity, so it was a valuable research to combine ZnO, CdO and graphene for the improvement of semiconductor catalysts. In the present study, ZnO/CdO nanoparticles were synthesized and immobilized on the surface of the reduced graphene oxide (rGO) *via* hydrothermal method. The sonocatal-

ytic activity of the as-prepared nanocomposites was studied related to the degradation of MEF, azo dyes and 4-NA. A series of parameters such as the combination ratio of ZnO/CdO nanoparticles and the reduced graphene oxide, the ultrasonic power, the dosage of catalyst and the initial concentration of MEF were optimized. Based on the results, the remarkably high activity of the as-prepared nanocomposites in the degradation of MEF, MO, RhB and 4-NA under ultrasonic irradiation was observed.

EXPRIMENTAL

Instruments and reagents

All materials were of a commercial reagent grade. FT Infrared (FT-IR) spectra were obtained from Bruker tensor 27DTGS. UV-Vis spectra were recorded on Lambda 35 spectrophotometer. XRD pattern was recorded by Jeol JDX-8030 with Cu k_α radiation (λ = 1.54 Å) in the 2θ range of 10–80°. The morphology, particle size, elements distribution and energy dispersive spectroscopy (EDS) of samples were observed by a scanning electron microscopy (SEM, KYKY-EM3200) and a transmission electron microscope (TEM, Zeiss-EM10C-(100 kV), Germany). Ultrasonic experiments were done on an ultrasonic processor, Chrom Tech Korea. Diffuse reflectance spectroscopy (DRS) was carried out on Avantes (Ava Lamp-DH-S Ava spec 2048- Tec).

Synthesis of graphene oxide (GO)

GO was synthesized from purified natural graphite powder via a modified Hummers method according to the literature.[34]

Synthesis of ZnO/CdO nanoparticles

ZnO/CdO nanoparticles were synthesized via template assisted route, according to the literature.[28] Details are available in Supplementary material to this paper.

Synthesis of ZnO/CdO/reduced graphene oxide (the nanocomposites)

A series of ZnO/CdO/reduced graphene oxide nanocomposites from 0 to 15 % were prepared by changing the amount of added ZnO/CdO in the process and labelled as ZnO/CdO/ /reduced graphene oxide (0/100), ZnO/CdO/reduced graphene oxide (5/100), ZnO/CdO/reduced graphene (10/100) and ZnO/CdO/reduced graphene oxide (15/100). The typical route of ZnO/CdO/reduced graphene oxide composites synthesis, when the mass ratio of ZnO/CdO/ /reduced graphene oxide is 10/100, for example, is as follows: 0.21 g of graphene oxide was dispersed in 30 mL of deionized water by sonication for 1 h. Then 20 mL of deionized water containing 0.02 g of as-synthesized ZnO/CdO nanoparticles was slowly added into the GO suspension. The mixture was sonicated for another 1 h, then 20 mL of $N_2H_4.H_2O$ was added into the above system and the solution was then sealed in a 100 mL teflon lined stainless steel autoclave for hydrothermal reaction at 180 °C for 8 h. After the autoclave was cooled down to room temperature, the ZnO/CdO/reduced graphene oxide product was collected, washed with water several times and dried at 60 °C for 10 h. The pure reduced graphene oxide was synthesized in the absence of ZnO/CdO nanoparticles.

Adsorption and sonocatalytic studies

1.2 g/L of as-prepared ZnO/CdO/reduced graphene oxide was added into 25 mL MEF, RhB, MO and 4-NA aqueous solution with concentration of 10 mg/L. After completely dispersed, the suspension was stirred in the dark to reach the adsorption/desorption equilibrium.

The temperature was fixed to be 25 °C with water bath. By the observations of UV–Vis spectrum, it was clear that the absorption spectrum of organic pollutants reached almost a constant value after 30 min. Then, the ultrasonic waves were applied for degradation. At different time intervals, 1 mL of solution was withdrawn from the reaction mixture and the concentration of the solutions was measured using UV–Vis spectrometer. UV–Vis spectral changes of substrates in the presence of ZnO/CdO/reduced graphene oxide nanocomposites were studied as a function of time under ultrasonic irradiation.

To investigate the effect of the ZnO/CdO/reduced graphene oxide, some experiments were performed to make sure that the degradation of the organic pollutants occurred as a result of the catalytic activity of the ZnO/CdO/reduced graphene oxide, and not because of the ultrasound or adsorption only. The degradation of the organic pollutants was studied: 1) with only ultrasound, 2) with ZnO/CdO nanoparticles, 3) with rGO and (4) with ZnO/CdO/reduced graphene oxide nanocomposites.

Evaluation of reactive oxygen specious (ROS), and Determination of the kind of ROS

Details are available in Supplementary material.

RESULT AND DISCOSSION

Structure and properties characterization

Fig. 1 shows the XRD spectra of graphene oxide, rGO and the as-synthesized nanocomposites. In Fig. 1a the diffraction peak at 2θ = 10.1° can be indexed to (002) crystallographic plane of graphene oxide.[35] In the XRD pattern of rGO nanosheets, the disappearance of the peak at 2θ = 10.1°, confirms that the graphite oxide has been flaked to rGO.[24] Also, rGO exhibited the broad peak at 24.6 which correspond to (002) plane. As can be seen in Fig. 1c the main dom-

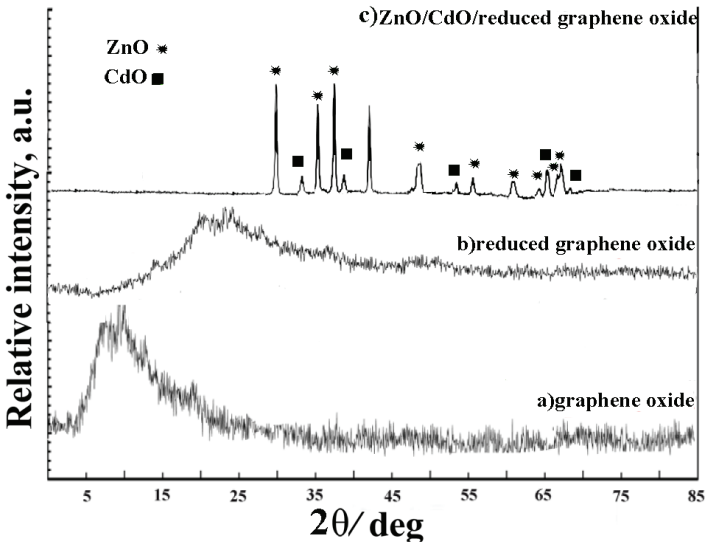

Fig. 1. XRD pattern of: a) graphene oxide, b) rGO and c) ZnO/CdO/reduced graphene oxide.

inant peaks for ZnO were identified at 2θ 31.8, 35.0, 36.2, 48.4, 56.2, 63.4, 66.1, 67 and 68.0° which can be indexed as (100), (002), (101), (102), (110), (103), (200), (112) and (201) associated to the diffraction of hexagonal wurtzite phase (JCPDS 79-0208). The peaks at 2θ 33, 38.6, 55.7, 66.5 and 69° can be indexed to (111), (200), (202), (311) and (222) crystallographic planes of cubic structure of CdO (JCPDS 65-2908).

Fig. 2a shows ZnO/CdO nanoparticles with the size around (15-80 nm). As shown in Fig. 2b and c, the ZnO/CdO nanoparticles are attached to the surface of the graphene nanosheet. The slight agglomeration of the nanoparticles was observed. The elemental composition was analyzed by an energy dispersive spectrometer (EDS) spectrum equipped with SEM. The EDS (Fig. 2d) analysis shows the presence of zinc (26.2 %) along with cadmium (12.1 %), carbon (42.9 %) and oxygen (18.8 %), which are the main elements for catalytic activity of the as-prepared nanocomposites.

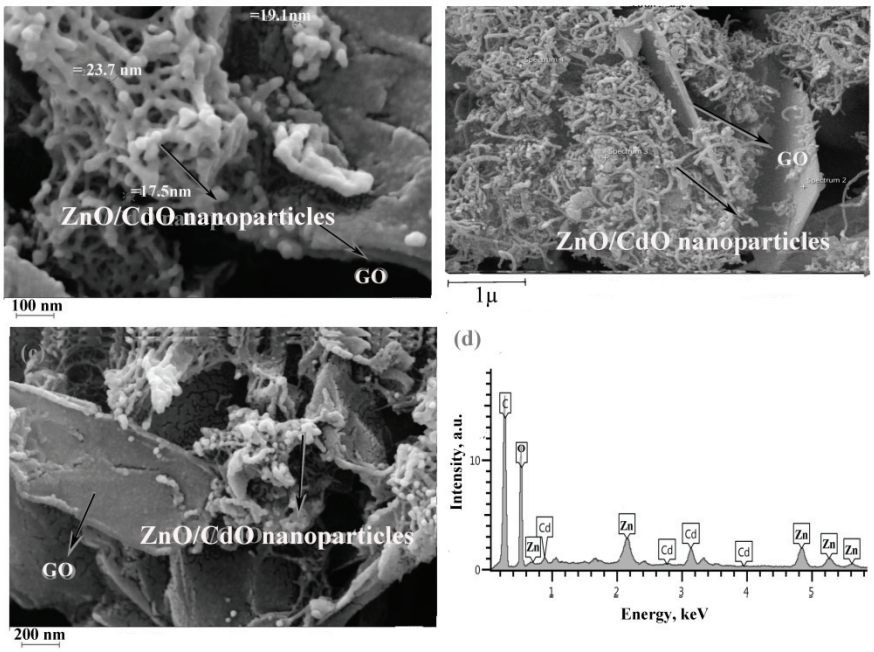

Fig. 2. SEM images of ZnO/CdO nanoparticles on reduced graphene oxide with different magnifications; EDX spectrum of ZnO/CdO/reduced graphene oxide.

The TEM images of ZnO/CdO/reduced graphene oxide (10/100) are shown in Fig. 3(a-c). As can be seen, the ZnO/CdO nanoparticles distributed on the surface of GO. Some of the nanoparticles have hexagonal morphology.

The FTIR spectra of GO exhibits the characteristic peaks as follows: the strong and broad absorption band at 3400 cm^{-1} originates from the stretching

vibration of O–H. The peaks at 1720, 1635, 1170 and 1060 cm^{-1} are attributed to the stretching vibrations of C=O, C=C, C–O–C and C–O. The FTIR spectrum of the rGO shows absorption band at 1635 cm^{-1} due to the C=C stretching vibration. In the FTIR spectrum of the as prepared nanocomposites, the absorption at 1720, and 1170 cm^{-1} has decreased, the absorption at 1060 cm^{-1} has vanished and the characteristic peak at 1635 cm^{-1} has not changed. The absorption band around 464 cm^{-1} is assigned to Cd–O.[28] The absorption band at 577 cm^{-1} can be assigned to Zn–O vibration.[36] The decreasing oxygen containing groups (C=O and C–O–C) and vanishing (C–O) in the FTIR spectra of the as-prepared nanocomposites is indicative of anchored ZnO/CdO nanoparticles on the surface of rGO. This phenomenon could provide enough adhesion strength to inhibit the aggregation and the loss of ZnO/CdO nanoparticles during sonocatalytic process and excellent stability (Fig. S-1 of the Supplementary material).

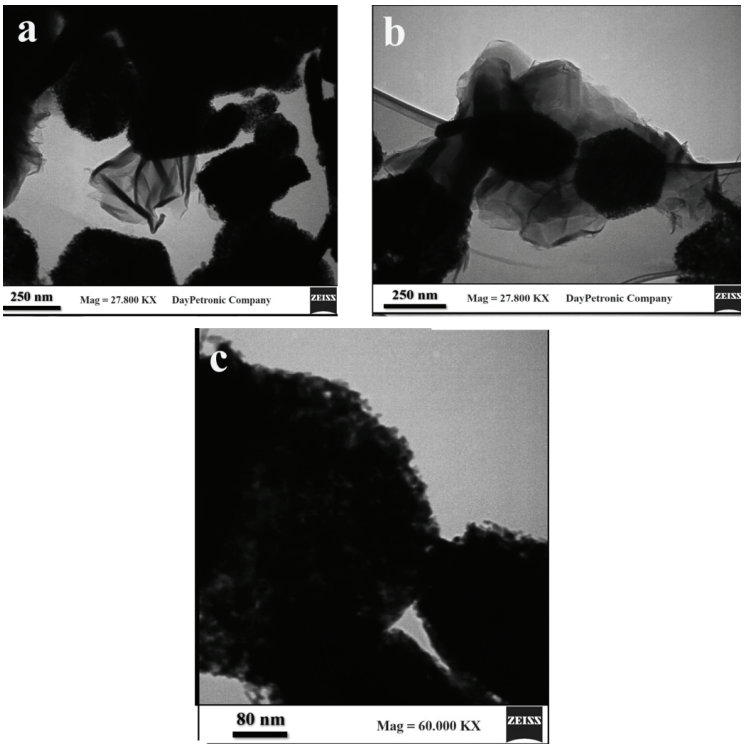

Fig. 3. TEM images of ZnO/CdO nanoparticles on reduced graphene oxide with different magnification (a–c).

Fig. S-2 of the Supplementary material shows the absorption spectra of GO, ZnO/CdO nanoparticles and ZnO/CdO/reduced graphene oxide. In the absorption spectra of GO, the absorption peak at 270 nm is assign to the π–π* transition of

aromatic C–C band, which has red shift in the ZnO/CdO/reduced graphene oxide. Also, in Fig. S-2c, the disappearance of a shoulder peak at 300 nm (the n–π* transition of C=O band) can be seen. Moreover the absorption intensity is significantly increased in the whole visible region.

Adsorption properties of the as-prepared nanocomposites

From Fig. S-3 of the Supplementary material, it can be noticed that, after 30 min, 30 % of MEF, 23 % of RhB, 25 % of MO and 33 % of 4-NA were adsorbed. By the observations it was clear that after 30 min, the absorption spectrum of the organic pollutants reached almost a constant value. The percentage of the organic pollutant degradation (*Deg* / %) was calculated as follows:

$$Deg = 100\frac{c_0 - c_f}{c_0} \quad (1)$$

where c_0 and c_f are the initial and final organic pollutants concentrations, respectively.

Sonocatalytic properties of the as-synthesized nanocomposites

Figure 4 shows the sonocatalytic degradation of the organic pollutants under different conditions. *i*) With only ultrasound irradiation, Fig. 4 indicates that little

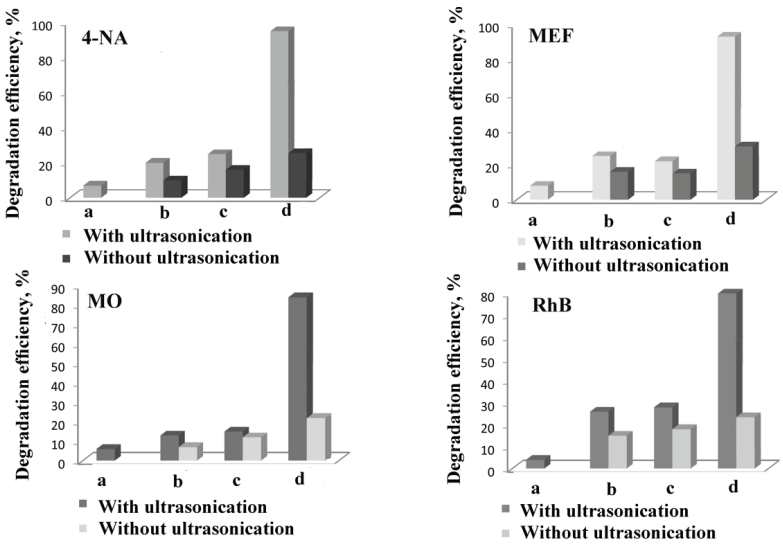

a) only ultrasonication, b)ZnO/CdO nanoparticles, c) rGO, d)ZnO/CdO/reduced graphene oxide

Fig. 4. Comparing the degrdation efficiency in different conditions: in the presence of: a) only ultrasound, b) ZnO/CdO nanoparticles, c) rGO and d) ZnO/CdO/reduced graphene oxide; reaction conditions for all of experiments: initial concentration of MEF, 4-NA and azo dyes 10 mg/L, volume of solution: 25 mL, reaction time: 120 min, catalyst amount (ZnO/CdO nanoparticles, rGO, the as-prepared nanocomposites: 1.2 g/L) and pH 7.5.

changes are observed on the degradation efficiency of the organic pollutants after only ultrasonic irradiation. It was found that the substrates are stable and cannot be simply degraded by the ultrasonic irradiation. *ii*) With ZnO/CdO nanoparticles, it is obvious that ZnO/CdO nanoparticles show the enhanced sonocatalytic efficiency (Fig. 4). The synergetic effects of CdO and ZnO enhanced the degradation efficiency, however due to the agglomeration of small nanoparticles, the degradation efficiency cannot proceed to high level. *iii*) With rGO, as can be seen in Fig. 4, due to the extraordinary properties of graphene, degradation efficiency to a certain level occurs. However, a single layer of graphene has strong tendency of agglomeration into multilayer graphite through strong π–π stacking and van der Waals interaction. *iv*) With the as-prepared nanocomposites, Fig. 4 indicates that the highest degradation efficiency of substrates was observed in presence of the as-prepared nanocomposite and the ultrasonic irradiation together. The degradation efficiency increased almost linearly with the increasing ultrasound irradiation time. Thus it gives us an insight into the sonocatalysis of organic pollutants by ZnO/CdO/reduced graphene oxide is powerful and efficient in dark state.

Fig. S-4a–d shows that the max absorption peak of MEF (217 nm), RhB (511 nm) and MO (465 nm) and 4-NA (379 nm) decreased gradually as the reactions proceeded in 30, 60, 90 and 120 min after the beginning under ultrasonic irradiation. Other peak was not observed which indicated that no by-product was produced.

Effects of the reactive oxygen species

According to the method of oxidation extraction photometry (OEP) [26] ROS could be detected by UV–VIS absorption spectrum. The ROS with great oxidizing ability can oxidize DPCI in to 1,5-diphenylcarbazone (DPCO). DPCO shows strong absorption at 563 nm. Fig. 5 shows absorption of DPCO, in different conditions.

From the intensity of absorbance of DPCO (Fig. 5), it can be derived that the quantity of generated ROS in the presence of ZnO/CdO/reduced graphene oxide is higher than under other conditions.

Effects of different parameters on sonocatalytic reaction

To investigate different parameters on sonocatalytic reaction, degradation of MEF was chosen as a model reaction.

Optimizing Combination ratio of ZnO/CdO/ reduced graphene oxide

A series of ZnO/CdO/reduced graphene oxide nanocomposites were prepared. The prepared composites were applied in degradation of MEF as a model reaction and the degradation ratio was calculated with c_e/c_0, where c_0 is the initial concentration and c_e is the concentration of MEF at different times. Fig. S-5 of

the Supplementary material shows the time profile of c_e/c_0 using the main absorption peak of MEF (217 nm in supplementary under irradiation). As evident, ZnO/CdO/reduced graphene oxide (5/100), ZnO/CdO/reduced graphene oxide (10/100) and ZnO/CdO/reduced graphene oxide (15/100) samples exhibited the improved sonocatalytic activity when compared to that of pure ZnO, CdO and rGO. Also, Fig. S-5 indicates an obvious advantage of ZnO/CdO/reduced graphene oxide (10/100).

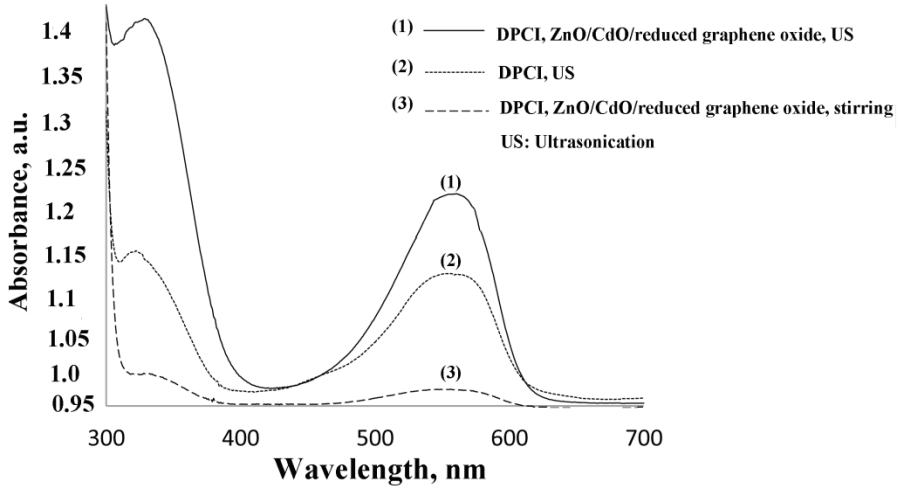

Fig. 5. UV–VIS spectra of DPCO in different condition. Experimental condition: ([DPCI] = = 1.0×10^{-2} mol/L, [ZnO/CdO/reduced graphene oxide] = 1.2 g/L and ultrasonic time: 45 min.

Effect of ZnO/CdO/reduced graphene oxide dosage

The dosage of the catalyst plays an important role in sonocatalytic degradation. Four different amounts of catalyst (0.3, 0.6, 0.9 and 1.2 g/L) were considered. With the increasing dosage of the as-prepared nanocomposite, the active sites of catalyst were increased. Thus more radicals were produced and the degradation efficiency was increased. Fig. S-6 of the Supplementary material presents the results of the experiments, the 1.2 g/L catalyst has shown maximum removal efficiency (93 %).

Effect of initial concentration of organic pollutant

To study the effects of the initial concentration of an organic pollutant on the sonocatalytic reaction, four different amounts of initial concentration of MEF (5, 10, 15 and 20 mg/L) were considered. Fig. S-7 shows that, with the increase of the initial concentration of MEF, the number of the MEF molecules is increased, whereas the number of hydroxyl radicals is constant. More hydroxyl radicals are required for the degradation of all of the molecules, therefore the degradation

efficiency is decreased. The results show that the initial concentration of MEF (10 mg/L) is suitable.

Effect of ultrasonic power

Fig. S-8 of the Supplementary material shows that with changing the ultrasonic power from 200 to 1200W/L, the acoustic cavitation is increased, therefore more hydroxyl radicals are produced and the degradation efficiency is increased. Hence the ultrasonic power is chosen to be 1200W/L.

Fig. S-9 of the Supplementary material shows the removal efficiency of the nanocomposite in optimized conditions. With the increasing reaction time, the removal efficiency increased linearly for all substrates. After the end of 120 min, under ultrasonic irradiation, MEF (93.0 %), MO (84.0 %), RhB (80.0 %) and 4-NA (95.0 %) were removed by the as-synthesized nanocomposites.

The kinetic study of the sonocatalytic reaction

For the sonocatalytic reaction of MEF, 4-NA and azo dyes, an approximately linear correlation of ln c_0/c *vs*. time is observed (Fig. 6). So, the sonocatalytic reaction is of the pseudo first order. The k_{app} values of rate of the sonocatalytic degradation are listed in Table I. The results show that the k_{app} value of MEF sonocatalytic degradation is higher than the other substrates.

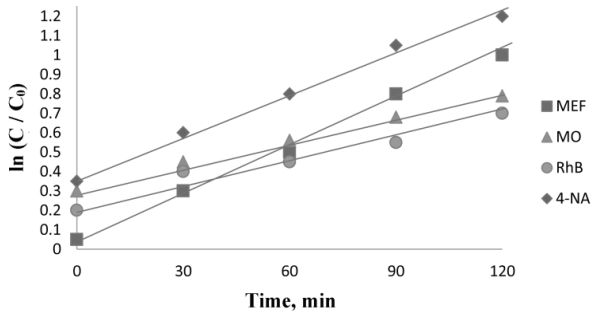

Fig. 6. The pseudo first order kinetics of sonocatalytic reactions of MEF and azo dyes under ultrasonic irradiation.

TABLE I. Rate coefficient of sonocatalytic reactions

Substrate	k_{app} / 10^{-3} min^{-1}
4-NA	7.1
MEF	8.0
MO	4.0
RhB	3.8

Sonocatalytic mechanism of as-prepared nanocomposites

Figure 7 illustrates the electron transfer mechanism in the sonocatalytic degradation of the organic pollutants. The enhanced degradation was achieved in

the presence of ZnO/CdO/reduced graphene oxide. It can be attributed to the fact that the presence of ZnO/CdO/reduced graphene oxide in the liquid medium enhances the formation of the reactive radicals such as $H^{\bullet}$ and $^{\bullet}OH$ (Eq. (3)) through the pyrolysis of water. Also, when the ZnO/CdO/reduced graphene is irradiated by ultrasonication, both CdO and ZnO semiconductors are excited and the electrons are excited from the valence band to the conduction band, forming the electron-holes pairs.[37–41] The energy band gap of the as-synthesized nanocomposite is 1.5 eV, calculated with DRS spectra of ZnO/CdO/reduced graphene oxide using Tauc relation:

$$\alpha h\nu = A(h\nu - E_g)^{m/2} \quad (2)$$

where α is the absorption coefficient and $h\nu$ is the frequency of photons. A is the proportionality constant and m = 4. Since the conduction bands of CdO and ZnO are very close together, electrons are injected from the conduction band of CdO into the conduction band of ZnO. This process can lead to high concentration of electrons in the conduction band of ZnO and to the charge separation. Afterwards the electrons can easily transfer to rGO due to the good conductivity of rGO, which can effectively improve the separation of sonogenerated e^{-}–h^{+} pairs enhancing the efficiency of the sonocatalytic degradation. The electrons can combine with O_2 in solution to form the strong oxidative species $^{\bullet}O_2^-$ on the other hand some of the excited holes at the valence band of ZnO would transfer to the valence band of the CdO *via* graphene. Furthermore, h^{+} can react with the surface adsorbed H_2O to produce $^{\bullet}OH$ or directly oxidize organic pollutants to CO_2, H_2O and some other small molecules.

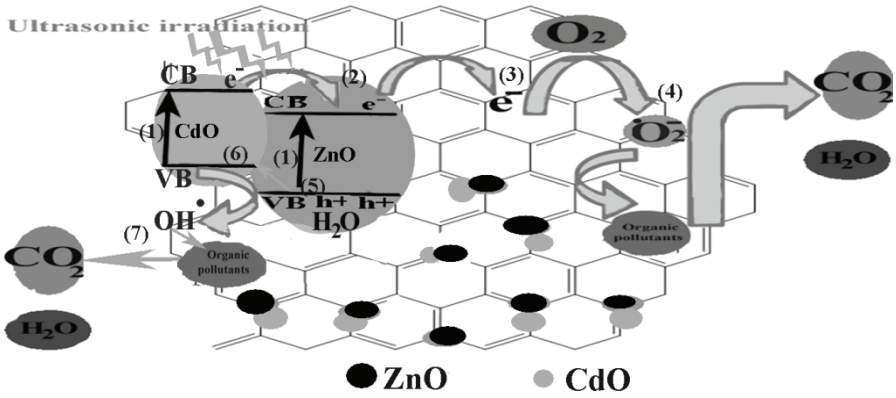

Fig. 7. Sonocatalytic degradation mechanism for the organic pollutants over ZnO/CdO/reduced graphene oxide composite under ultrasonic irradiation.

In order to determine what is the dominant controlling mechanism of the sonocatalytic degradation (pyrolysis or free radical attack), the effects of the

scavengers on the sonocatalytic degradation were considered. For this purpose MEF degradation was chosen as a model reaction. The experiments were carried out using carbonate, iodide as inorganic scavengers and *tert*-butyl alcohol (T-butanol), as an organic scavenger. As it is shown in Fig. S-10 of the Supplementary material, after adding CO_3^{2-}, I^- and T-butanol as radical scavengers, degradation efficiency of MEF was decreased from 93 to 80, 76 and 58 % at the reaction time of 120 min, respectively. Among the scavengers, T-butanol has led to the greatest reduction in degradation efficiency. The results suggest, the degradation of MEF was mainly done by $^{\bullet}O_2^-$ and $^{\bullet}OH$. Thus it can be concluded that the free radical attack is the dominant controlling mechanism of the sonocatalytic degradation of MEF.

In order to determine the main reactive oxidant species, the trapping experiment using L-His, Thiore and VC as the quenching agents were carried out. Fig. S-11 of the Supplementary material clearly displays the addition of effective reducers. In general, L-histidine can quench the singlet molecular oxygen ($^1O_2$) and $^{\bullet}OH$, thiourea quenches the hydroxyl radical and vitamin C can quench most kinds of radicals.[42,43]

As can be seen in Fig. S-11, with ZnO/CdO/reduced graphene oxide and ultrasonication, the absorbance of DPCO at 563 nm was decreased by 66, 74 and 81 % in presence of L-His, thiourea and vitamin C (VC), respectively. The use of these scavengers produces $^1O_2$ and $^{\bullet}OH$. Thus, the absorbance of DPCO is decreased. It is found that $^{\bullet}OH$ and $^1O_2$ are major kinds of ROS with ultrasonic irradiation. Based on the above results, the mechanisms of the ultrasonic wave's absorption, charge transfer, and the reaction pathways are as follows):

$$H_2O + \text{Ultrasound} \rightarrow {}^{\bullet}OH + {}^{\bullet}H \quad (3)$$

$$\text{Ultrasound} \rightarrow h\nu \quad (4)$$

$$\text{ZnO/CdO} + \text{Ultrasonic irradiation} \rightarrow \text{ZnO/CdO}\ (h^+ + e^-) \quad (5)$$

$$\text{ZnO/CdO}\ (e^-) + \text{rGO} \rightarrow \text{ZnO/CdO} + \text{rGO}\ (e^-) \quad (6)$$

$$e^- + h^+ \rightarrow \text{Heat or } h\nu \quad (7)$$

$$h^+ + H_2O \rightarrow {}^{\bullet}OH + H^+ \quad (8)$$

$$e^- + O_2 \rightarrow O_2^{\bullet-} \quad (9)$$

$$O_2^{\bullet-} + \text{Organic pollutants} \rightarrow CO_2 + H_2O + \text{Product} \quad (10)$$

$${}^{\bullet}OH + \text{Organic pollutants} \rightarrow CO_2 + H_2O + \text{Product} \quad (11)$$

In order to justify the superior activity of ZnO/CdO/reduced graphene oxide, the present study is compared with some others from literature for the degradation of MO, RhB and MEF. The results are depicted in Table II. It is worth noting that few studies have focused on the degradation of more than three pollut-

ants using semiconductor oxide nanoparticles and graphene during sonocatalytic reaction. In our case, four organic pollutants were removed efficiently using ZnO/CdO/reduced graphene oxide in the degradation.

TABLE II. Comparison of sonocatalytic performances of ZnO/CdO/reduced graphene oxide and some of other catalysts for removal of MEF, RhB, MO and 4-N

Entry	Catalyst	Degradation route	Pollutant (Degradation, %)	Reaction time, min	Ref
1	ZnO-graphene	Visible light irradiation	MO (87)	180	[44]
2	Supported CuO-ZnO	Hg lamp(55W)	MEF (67)	200	[45]
3	Activated carbon	UV irradiation+ ozone	MEF (60)	120	[46]
4	SnO_2-reduced graphene oxide	Visible light irradiation	RhB (79)	175	[47]
5	$H_3P_{12}W_{40}/TiO_2$	UV irradiation (250W)	4-NA (95)	120	[48]
6	TiO_2-coated censpheres	Solar light irradiation	4-NA (63)	180	[49]
7	α-Fe_2O_3	Xenon arc lamp(300 W)	RhB (79)	140	[50]
8	Nickel hydroxide	Different speed of agitation (300–500 rpm)	MO (80)	120	[51]
9	ZnO/CdO/reduced graphene oxide	Ultrasonic irradiation	MO(84), RhB(80), 4-NA(95) and MEF(93)	120	This work

Reusability test

For practical applications, the reusability test on ZnO/CdO/reduced graphene oxide catalyst was carried out. Figure 8 shows that in optimized conditions for MEF, azo dyes and 4-NA solution, the stability of the catalyst was excellent. The sonocatalytic degradation ratios of MEF, azo dyes and 4-NA showed slight decrease during 4 recycle times.

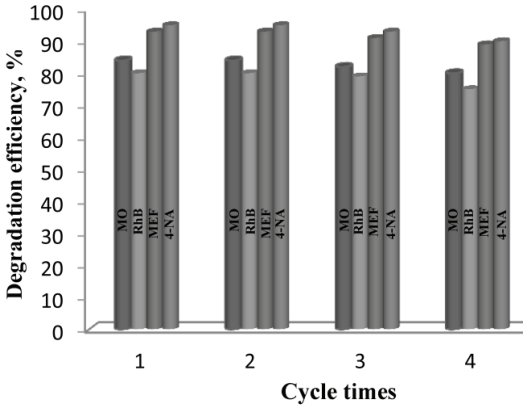

Fig. 8. The catalytic performance of as--synthesized nanocomposite for 4 successive cycles. Reaction conditions: the cleaned ZnO/CdO/reduced graphene oxide nanocomposites were immersed in ethanol for 6h and rinsed with deionized water and then dried at 70 °C. ZnO/CdO/reduced graphene oxide (10/100): 1.2 g/L, initial concentration of MEF, azo dyes, 4-NA: 10 mg/L, ultrasonic power 1200W/L. pH 7.5

CONCLUSIONS

The ZnO/CdO/reduced graphene oxide nanocomposites was-prepared by the hydrothermal method characterized, by FTIR, XRD, EDX, DRS, SEM, TEM and UV–Vis techniques. The sonocatalytic properties of as-prepared nanocomposites were evaluated in degradation of MEF, 4-NA and azo dyes under ultrasonic irradiation. The parameters which affect the sonocatalytic degradation such as the dosage of catalyst, the initial concentration of organic pollutant and the ultrasonic power were optimized using MEF degradation as a model reaction. Based on the results in the sonocatalytic degradation, the degradation efficiency after 120 min for MEF, 4-NA, RhB and MO are 93.0, 95.0, 80.0 and 84.0 %, respectively. The results of ROS experiments verified that the free radical attack is the dominant controlling mechanism of the sonocatalytic degradation of the organic pollutants.

Moreover, the kinetics of the sonocatalytic degradation follows the pseudo first order kinetics. The prepared nanocomposites can be reused for several times with very slight decrease in the degradation efficiency. The significantly enhanced sonocatalytic efficiency of ZnO/CdO/reduced graphene oxide rather than the one of ZnO/CdO nanoparticles and rGO (in the absence of ZnO/CdO nanoparticles), is attributed to the triple function of the ZnO/CdO/reduced graphene oxide, which is: 1) the close contact between ZnO, CdO and rGO, 2) the ultrafast electron transfer from ZnO/CdO nanoparticles to rGO, which significantly hinders the recombination of charge carriers and 3) the activation of the organic pollutant molecules via π–π interaction between the organic pollutants and rGO. Considering the cheap raw materials, the recoverable and excellent sonocatalytic activity, the ZnO/CdO/reduced graphene oxide can be potentially applied in the water purification industry.

SUPPLEMENTARY MATERIAL

Experimental details and additional data and analyses are available electronically at the pages of journal website: http://www.shd.org.rs/JSCS/, or from the corresponding author on request.

Acknowledgments. The authors thank Alzahra University for all the support.

ИЗВОД

РЕДУКОВАНИ ГРАФЕН-ОКСИД СА НАНОЧЕСТИЦАМА ZnO/CdO И ЊЕГОВЕ КАТАЛИТИЧКА СВОЈСТВА ПРИ РАЗГРАДЊИ ОРГАНСКИХ ЗАГАЂИВАЧА

HODA MIRZAZADEH и MARYAM LASHANIZADEGAN

Department of Chemistry, Faculty of Physics and Chemistry, Alzahra University, P. O. Box 1993893973, Tehran, Iran

Наночестице ZnO/CdO су нанесене на редуковани графен-оксид (ZnO/CdO/редуковани графен-оксид) хидротермалним поступком. Структура и морфологија испитани су техникама FTIR, UV–Vis, XRD, EDX, DRS, SEM и TEM. Оцењена су сонокаталитичка својства ZnO/CdO/редукованог графен-оксида у деградацији мефенамичне киселине (MEF), метил-оранжа (MO), родамина (RhB) и 4-нитроаналина (4-NA). 120 min након

почетка реакције измерена је висока ефикасност разградње азо-боја (MO: 84 %, RhB: 80 %), MEF: 93 % и 4-NA: 95 %. Проучени су ефекти фактора као што је дозирање ZnO/ /CdO/редукованог графен-оксида, почетна концентрација органског загађивача, снага ултразвука и присуство инхибитора реактивних врста кисеоника (ROS) на ефикасност разградње. Нађено је да је присуство инхибитора умањује ефикасност сонокаталитичке разградње. Ова истраживања указују на то да готови припремљени нанокомпозити испољавају знатно већу каталитичку активност него ZnO/CdO наночестице са редукованим графен-оксидом (rGO).

(Примљено 30. јуна, ревидирано 10. августа, прихваћено 11. августа 2017)

REFERENCES

1. C. G. Daughton, T. A. Ternes, *Environ. Health Perspect.* **107** (1999) 907
2. T. A. Ternes, M. Meisenheimer, D. McDowell, F. Sacher, H.-J. Brauch, B. Haist-Gulde, G. Preuss, U. Wilme, N. Zulei-Seibert, *Environ. Sci. Technol.* **36** (2002) 3855
3. O. Drzyzga, *Chemosphere* **53** (2003) 809
4. B. Soulet, A. Tauxe, J. Tarradellas, *Int. J. Environ. Anal. Chem.* **82** (2002) 659
5. L. J. Nadeau, J. C. Spain, *Appl. Environ. Microbiol.* **61** (1995) 840
6. M. M. Nassar, M. S. El-Geundi, *J. Chem. Technol. Biotechnol.* **50** (2007) 257
7. K. R. Ramakrishna, T. Viraraghavan, *Water Sci. Technol.* **36** (1997) 189
8. C. O'Neill, F. R. Hawkes, D. L. Hawkes, N. D. Lourenço, H. M. Pinheiro, W. Delée, *J. Chem. Technol. Biotechnol.* **74** (1999) 1009
9. T. Harifi, M. Montazer, *J. Mater. Chem., B* **2** (2014) 272
10. S. A. Vanalakar, V. L. Patil, N. S. Harale, S. A. Vhanalakar, M. G. Gang, J. Y. Kim, P. S. Patil, J. H. Kim, *Sensors Actuators, B: Chem.* **221** (2015) 1195
11. J. Yi, D. Lu, X. Li, S. Hu, W. Li, J. Lei, Y. Wang, *J. Solid State Electrochem.* **16** (2012) 443
12. B. Lim, M. Jiang, P. H. C. Camargo, E. C. Cho, J. Tao, X. Lu, Y. Zhu, Y. Xia, *Science* **324** (2009) 1302
13. A. Halder, S. Patra, B. Viswanath, N. Munichandraiah, N. Ravishankar, *Nanoscale* **3** (2011) 725
14. T. Yu, J. Zeng, B. Lim, Y. Xia, *Adv. Mater.* **22** (2010) 5188
15. K. S. Novoselov, *Science* **306** (2004) 666
16. X. Yang, A. Wolcott, G. Wang, A. Sobo, R. C. Fitzmorris, F. Qian, J. Z. Zhang, Y. Li, *Nano Lett.* **9** (2009) 2331
17. C. Hariharan, *Appl. Catal., A: Gen.* **304** (2006) 55
18. B. H. San, J. A. Kim, A. Kulkarni, S. H. Moh, S. R. Dugasani, V. K. Subramani, N. D. Thorat, H. H. Lee, S. H. Park, T. Kim, K. K. Kim, *ACS Nano* **8** (2014) 12120
19. Q. Xiang, J. Yu, M. Jaroniec, *Nanoscale* **3** (2011) 3670
20. X. Chen, Y. He, Q. Zhang, L. Li, D. Hu, T. Yin, *J. Mater. Sci.* **45** (2010) 953–960.
21. Y. Yang, L. Ren, C. Zhang, S. Huang, T. Liu, *ACS Appl. Mater. Interfaces* **3** (2011) 2779
22. Q.-P. Luo, X.-Y. Yu, B.-X. Lei, H.-Y. Chen, D.-B. Kuang, C.-Y. Su, *J. Phys. Chem., C* **116** (2012) 8111
23. T. Lv, L. Pan, X. Liu, T. Lu, G. Zhu, Z. Sun, *J. Alloys Compd.* **509** (2011) 10086
24. W. Han, L. Ren, X. Qi, Y. Liu, X. Wei, Z. Huang, J. Zhong, *Appl. Surface Sci.* **299** (2014) 12
25. M. Ahmad, E. Ahmed, Z. L. Hong, W. Ahmed, A. Elhissi, N. R. Khalid, *Ultrason. Sonochem.* **21** (2014) 761
26. L. Zhu, J. Chung, W.-C. Oh, *Ultrason. Sonochem.* **27** (2015) 252

27. X. Zhu, Y. Zhu, S. Murali, M. D. Stoller, R. S. Ruoff, *ACS Nano* **5** (2011) 3333
28. M. Lashanizadegan, H. Mirzazadeh, *J. Ceram. Process. Res.* **13** (2012) 389
29. P. K. Sahoo, B. Panigrahy, D. Bahadur, *RSC Adv.* **4** (2014) 48563
30. A. A. Ashkarran, B. Mohammadi, *Appl. Surface Sci.* **342** (2015) 112
31. M. Ristić, S. Popović, S. Musić, *Mater. Lett.* **58** (2004) 2494
32. J. Chang, V. V. Todkar, R. S. Mane, D. Ham, T. Ganesh, S. H. Han, *Phys., E: Low-Dim. Syst. Nanostruct.* **41** (2009) 1741
33. S. Kumar, A. K. Ojha, B. Walkenfort, *JPB* **159** (2016) 111
34. H. N. Tien, V. H. Luan, T. V. Cuong, B.-S. Kong, J. S. Chung, E. J. Kim, S. H. Hur, *J. Nanosci. Nanotechnol.* **12** (2012) 5658
35. A. F. De Faria, D. S. T. Martinez, S. M. M. Meira, A. C. M. de Moraes, A. Brandelli, A. G. S. Filho, O. L. Alves, *Colloids Surfaces, B: Biointerfaces* **113** (2014) 115
36. Z. Wang, H. Zhang, L. Zhang, J. Yuan, S. Yan, C. Wang, *Nanotechnology* **11** (2002) 11
37. M. Salavati-Niasari, F. Davar, M. Farhadi, *J. Sol-Gel Sci. Technol.* **51** (2009) 48
38. R. W. Matthews, *J. Phys. Chem.* **91** (1987) 3328
39. C. Petrier, A. Jeunet, J.-L. Luche, G. Reverdy, *J. Am. Chem. Soc.* **114** (1992) 3148
40. T. J. I. Edison, M. G. Sethuraman, *Spectrochim. Acta, A: Mol. Biomol. Spectrosc.* **104** (2013) 262
41. T. Ghosh, K. Ullah, V. Nikam, C. Y. Park, Z. Da Meng, W. C. Oh, *Ultrason. Sonochem.* **20** (2013) 768
42. C. Xiao-jun, X. U. Han-hong, W. Yu-jian, H. U. Shan, Z. Zhi-xiang, Z. Yao-mou, *Agric. Sci. China* **6** (2007) 458
43. S. ichiro Umemura, N. Yumita, K. Umemura, R. Nishigaki, *Cancer Chemother. Pharmacol.* **43** (1999) 389
44. J. Xu, Y. Cui, Y. Han, M. Hao, X. Zhang, *RSC Adv.* **6** (2016) 96778
45. A. Shirzadi, A. Nezamzadeh-Ejhieh, *J. Mol. Catal., A: Chem.* **411** (2016) 222
46. O. Gimeno, J. Rivas, A. Encinas, F. Beltran, *World Acad. Sci. Eng. Technol.* **4** (2010) 1104
47. J. Zhang, Z. Xiong, X. S. Zhao, *J. Mater. Chem.* **21** (2011) 3634
48. W. H. Huang, R. Liu, *Adv. Mater. Res.* **233**–**235** (2011) 967
49. P. K. Surolia, R. J. Tayade, R. V. Jasra, *Ind. Eng. Chem. Res.* **49** (2010) 8908
50. A. Umar, M. S. Akhtar, G. N. Dar, S. Baskoutas, *Talanta* **116** (2013) 1060
51. M. Saeed, S. Adeel, M. Ilyas, M. A. Shahzad, M. Usman, E. Haq, M. Hamayun, *Desalin. Water Treat.* **57** (2016) 12804.